- 1 To be submitted: Geoscientific Model Development
- 2 Development of a Model Framework for Terrestrial Carbon Flux Prediction: the Regional Carbon
- and Climate Analytics Tool (RCCAT) Applied to Non-tidal Wetlands
- 4 Ashley Brereton* ^{1,2}, Zelalem A Mekonnen¹, Bhavna Arora¹, William J. Riley¹, Kunxiaojia Yuan¹,
- 5 Yi Xu², Yu Zhang³, Qing Zhu¹, Tyler L. Anthony⁴, Adina Paytan²
- 6
- 7 Earth and Environmental Sciences Area, Lawrence Berkeley National Laboratory, Berkeley, CA,
- 8 USA¹
- 9 Department of Earth and Planetary Sciences, University of California at Santa Cruz, Santa
- 10 Cruz, CA, USA²
- 11 Earth and Environmental Sciences Division, Los Alamos National Laboratory, Los Alamos, New
- 12 Mexico, USA³
- 13 California Department of Water Resources, Sacramento, CA, USA⁴
- 14 *Corresponding author, ashbre@lbl.gov
- 15
- 16
- 17 Abstract
- Wetlands play a pivotal role in carbon sequestration but emit methane (CH_4) , creating
- 19 uncertainty in their net climate impact. Although process-based models offer mechanistic
- 20 insights into wetland dynamics, they require extensive site-specific parameterisation (e.g. soil
- 21 carbon profiles, pore-water chemistry, vegetation-specific model parameters), as well as high-
- 22 resolution hydrological and meteorological inputs that are often difficult to obtain outside of well-
- 23 instrumented research sites, which makes regional upscaling challenging. In contrast, data-
- 24 driven models provide a scalable alternative by leveraging available datasets to identify patterns
- and relationships, making them more adaptable for large-scale applications. However, their
- 26 performance can vary significantly depending on the quality and representativeness of the data,
- 27 as well as the model design, which raises questions about their reliability and generalizability in
- complex wetland systems. To address these issues, we present a data-driven framework for
- 29 upscaling wetland CO₂ and CH₄ emissions, across a range of machine learning models that
- 30 vary in complexity, validated against an extensive observational dataset from the Sacramento-
- 31 San Joaquin Delta. We show that artificial intelligence (AI) approaches, including Random
- 32 Forests, gradient boosting methods (XGBoost, LightGBM), Support Vector Machines (SVM) and
- Recurrent Neural Networks (GRU, LSTM), outperform linear regression models, with RNNs
- standing out, achieving an R² of 0.73 for daily CO₂ flux predictions compared to 0.64 for linear
- regression, and an R² of 0.53 for CH₄ flux predictions compared to 0.47 for linear regression.
- 36 Interestingly, linear regression performed better than random forest for methane flux, which
- 37 highlights the necessity for comparison. The, interannual variability is less well captured, with
- 38 annual mean absolute error of 176 gC m⁻² yr⁻¹ for CO₂ fluxes and 9 gC-CH₄ m⁻² yr⁻¹ for CH₄

- 39 fluxes. By integrating vertically-resolved atmospheric, subsurface, and spectral reflectance
- 40 information from readily available sources, the model identifies key drivers of wetland CO₂ and
- 41 CH₄ emissions and enables regional upscaling. These findings demonstrate the potential of Al
- 42 methods for upscaling, providing practical tools for wetland management and restoration
- 43 planning to support climate mitigation efforts.

45

49

52

58

1. Introduction

Wetlands provide a wide array of ecological, economic, and environmental benefits (Costanza

et al., 2014). They play a crucial role in biodiversity conservation, water purification, flood

48 control, and climate regulation (Grande et al., 2023; Sharma and Singh, 2021). Significant

attention has been recently given to wetland restoration due to their ability to sequester carbon

from the atmosphere (Lolu et al., 2020; Upadhyay et al., 2020). These ecosystems are highly

effective at storing carbon in their soils because the anaerobic conditions in waterlogged soils

suppress organic matter decomposition, allowing carbon to accumulate over time (Mitsch and

Gosselink, 2015a). However, wetlands can also be significant sources of CH₄, a potent

54 greenhouse gas (Brix et al., 2001), leading to potentially net positive effects of wetlands on

55 climate warming. The most accurate way to determine the carbon balance in natural

56 ecosystems is through direct and continuous measurements of carbon and GHG sources and

57 sinks (Baldocchi et al., 2001). This involves monitoring carbon dynamics using techniques such

as eddy covariance (EC) towers (Aubinet et al., 2012), soil carbon stock assessments (Harrison

59 et al., 2011), and lateral carbon transport measurements (Ciais et al., 2008). However, these

60 measurements are time-consuming to carry out, costly, and require specialized instruments and

expertise, limiting their application to a few representative sites globally (Hill et al., 2017; Kumar

62 et al., 2017). The Ameriflux network offers roughly 500 EC sites comprising about 3600 site

years of data, monitoring carbon fluxes across various ecosystems such as forests, grasslands,

and wetlands (Pastorello et al., 2020). Eddy-covariance site footprints range in scale and are

65 typically determined by the sensor height and atmospheric turbulence (Chu et al., 2021). Data

from these Ameriflux sites could potentially be upscaled and used for estimating fluxes from

67 non-monitored sites to obtain regional assessments of carbon balance for various ecosystem

types, including wetlands.

In this study, we focus on nontidal wetlands due to the presence of a cluster of EC towers in a

70 small region located in the Sacramento-San Joaquin Delta, including three sites, each with over

a decade of continuous data. Reported sequestration rates in wetlands vary widely, influenced

by factors such as climate, vegetation, and management. For instance, reported sequestration

73 rates range from as low as 26 gC m⁻² yr⁻¹ in boreal rain-fed bogs (Villa and Bernal, 2018) to as

high as 797 gC m⁻² yr⁻¹ in constructed wetlands with emergent *Phragmites* in the Netherlands

75 (de Klein and van der Werf, 2014). Similarly, temperate wetlands in central Ohio exhibit a wide

76 range of carbon sequestration rates depending on vegetation: forested depressional wetlands

dominated by *Quercus palustris* sequester up to 473 gC m⁻² yr⁻¹, while marshes dominated by

78 Typha sequester around 210 gC m⁻² yr⁻¹ (Bernal and Mitsch, 2012). In Victoria, Australia,

79 freshwater marshes show varying sequestration rates from 91 gC m⁻² yr⁻¹ in shallow marshes to

80 230 gC m⁻² yr⁻¹ in permanent open freshwater wetlands (Carnell et al., 2018). More relevant to 81 this study, in the San Francisco Bay-Delta region, nontidal managed wetlands dominated by 82 Schoenoplectus and Typha species sequester carbon at rates of approximately 355 ± 249 gC-83 CO₂ m⁻² yr⁻¹. This estimate is based on direct calculations using Ameriflux data from sites with 84 over a decade of observations (US-Myb, US-Tw1, and US-Tw4). For this calculation we used 85 full-year annual averages and their corresponding standard deviation to the annual mean, to 86 highlight the significant inter-annual variability, with the standard deviation close to the mean. 87 The unit reported for these Delta sites is in gC-CO₂ m⁻² yr⁻¹, as the EC tower directly detects CO₂ exchange, which is convenient for GHG assessment purposes. It is worth noting that, at 88 89 these sites, some years were a net CO₂ source, due to site-specific disturbances such as 90 caterpillar infestations, drought, or when vegetation cover was fully established (Anderson et al., 91 2018; Knox et al., 2017; Rey-Sanchez et al., 2021). See table S1 for more detailed information 92 and references therein.

93

94

95

96

97

98

99

100

101

102

103

104

105

106

107

108

109

110

111

112

113

114

115

116

Although CO₂ balance (photosynthesis minus community respiration) is an important component of carbon sequestration, in many wetland systems sequestration benefits are counterbalanced by CH₄ emissions, a potent greenhouse gas, with a warming potential 27 times higher than CO₂ (Lee et al., 2023) that can often offset climate mitigation efforts. CH₄ emission rates also vary substantially over time and across wetlands, from as low as 0.23 gC-CH₄ m⁻² yr⁻¹ in saltwater zones of estuarine environments (Abril and Iversen, 2002) to as high as 270 gC-CH₄ m⁻² yr⁻¹ in certain freshwater wetlands (Knox et al., 2021). For example, restored freshwater wetlands in Maryland dominated by grasses and sedges emit around 142 gC-CH₄ m⁻² yr⁻¹ (Stewart et al., 2024). Tropical wetlands in Costa Rica exhibit some of the highest emissions, with isolated and floodplain wetlands releasing between 220 and 263 gC-CH₄ m⁻² yr⁻¹ (Mitsch et al., 2013). The San Francisco Bay-Delta wetlands that have high carbon sequestration rates also release CH₄ at rates of 35 ± 13 gC-CH₄ m⁻² yr⁻¹ (direct measurements from the eddy covariance tower data (Arias-Ortiz et al., 2021)). See table S2 for further information and reference therein. This dual role of wetlands in both sequestering carbon and emitting CH₄ reveals the complex effect they have on the global greenhouse gas balance. Therefore, integrating CO₂ and CH₄ emissions is critical to assess the net climate benefits of wetland conservation and restoration initiatives.

To evaluate how wetlands contribute to the atmospheric radiation budget at larger scales, it is essential to quantify both GHG emissions and carbon sequestration, especially at sites where direct measurements are unavailable (Moomaw et al., 2018). Upscaling models serve this purpose by allowing estimation of sequestration and emission rates across larger spatial scales than those covered by the original data sources (Villa and Bernal, 2018) which provide GHG accounting and net climate benefit assessments for specific wetland sites (Nahlik and Fennessy, 2016). Moreover, it aids in targeting wetland restoration efforts that aim to optimize sequestration by identifying locations with the greatest potential for net carbon uptake.

Process-based models have traditionally been used to estimate sequestration and emissions (Mack et al., 2023; Zhang et al., 2002). Models such as DNDC (Li, 1996), DayCent (Parton et al., 1998), and *Ecosys* (Grant et al., 2017) have been applied to simulate biogeochemical processes in terrestrial ecosystems, including modeling CH₄ emissions, carbon balances, and

soil carbon and nitrogen cycling (Grant and Roulet, 2002; Weiler et al., 2018; Zhang et al.,

122 2002). While these models can elucidate the processes that play a role in carbon dynamics,

they require extensive mechanistic parameterization to accurately represent the interactions in

various ecosystems (Pastorello et al., 2020; Yin et al., 2023). This approach often necessitates

125 site-specific information and data collection, making implementation over vast areas challenging

126 (Saunois et al., 2024; Xu and Trugman, 2021). The extensive data needs associated with these

process-rich models showcase the need for alternative approaches that can effectively upscale

wetland emissions without such intensive resource demands.

127

133

145

161

Artificial Intelligence (AI) methods, such as machine learning and deep learning, have been widely applied in ecological modeling in recent years, alongside long-term, large-scale data

131 collection efforts (Perry et al., 2022). Recent deep learning applications have demonstrated

success in capturing the complex dynamics of carbon and methane fluxes in these systems

(Ouyang et al., 2023; Yuan et al., 2022, 2024; Zou et al., 2024). The availability of open-source

modeling platforms like TensorFlow and PyTorch has made advanced computational

techniques, such as neural networks, more accessible, enabling the rapid development and

deployment of a range of specialized modeling tasks (Xu et al., 2021). Despite several recent

137 studies demonstrating the potential of machine learning for large-scale carbon cycling in

wetland ecosystems, this remains a relatively young field. Moreover, carbon dynamics in

wetland ecosystems are temporally variable and inherently nonlinear, making them particularly

well-suited for testing machine learning approaches (Arora et al., 2019, 2022). We therefore

141 emphasize the importance of evaluating and comparing various approaches within this domain

142 and their potential for large-scale assessment.

143 A pervasive challenge in model development is the ability to balance complexity with

144 generalizability. While more complex models can capture nonlinear relationships, they also

increase the risk of overfitting, where the model performs well in the testing, but poorly on new

146 conditions (Hastie, 2009; Tashman, 2000). Furthermore, it is also important to use a robust

validation framework. For the application of upscaling, it is important that the model is able to

extrapolate spatially. For this purpose, a leave-one-site-out (LOSO) validation approach is

typically carried out, whereby the models are trained on data that excludes a single site, with the

excluded site data saved for model testing (Bodesheim et al., 2018; Tramontana et al., 2016). It

is also important to avoid data leakage, where information from the training set inadvertently

appears in the testing set (Kaufman et al., 2012), a risk posed when splitting temporally

adjacent data points that are close in value, potentially inflating performance statistics (Bergmeir

and Benítez, 2012; Kaufman et al., 2012). For example, daily rates of change relative to a

155 system where seasonal dynamics dominate, such as emissions of CH₄ emissions in vegetated

156 wetlands (Knox et al., 2021).

157 In this study, we introduce a model framework for coastal nontidal wetland CO₂ and CH₄

158 emissions using several 'off-the-shelf' models. These models are trained and validated against

observational data, and results are compared to find the most predictive model. The top

performing model is then used to upscale carbon sequestration and CH₄ emissions in nontidal

wetlands at regional scale. The San Francisco Bay-Delta serves as the area of interest, due to

its network of EC towers that have been operating for a relatively long time and relevance to

future wetland restoration efforts. We employ a suite of models, ranging widely in complexity: (1) linear regression; (2) Random Forests (Breiman, 2001), an ensemble method that constructs multiple decision trees to reduce overfitting; (3) gradient boosting techniques such as LightGBM (Ke et al., 2017) and XGBoost (Chen and Guestrin, 2016), which are scalable tree boosting systems able to handle complex nonlinear relationships and variable interactions; (4) Support Vector Machines (SVM) (Cortes, 1995), a kernel-based technique that can approximate nonlinear boundaries between data points and (5) the Recurrent Neural Network (RNN) such as the Long Short-Term Memory (LSTM) neural network (Hochreiter, 1997), an advanced model designed to process sequential data and capture non-linear interactions over long-term dependencies. We also test a model with similar but simpler architecture, the Gated Recurrent Unit (GRU) (Chung et al., 2014), which uses fewer parameters. Linear regressions serve as a baseline to assess the applicability of the more sophisticated methods. Random Forests have been used to upscale northern wetland methane emissions (Peltola et al., 2019), gradient boosting methods have demonstrated success in ecological modeling (Ding, 2024; Räsänen et al., 2021; Zou et al., 2024), and LSTM neural networks have been successfully applied to model CO₂ and CH₄ fluxes in ecosystems (Yuan et al., 2022, 2024; Zou et al., 2024). Our proposed framework is designed to provide transparency, easy determination of model practicality and applicability, and contextualisation to model performances by comparing to a baseline model (i.e. linear regression).

2. Methods

- Our ultimate aim is to establish a robust modeling framework for estimating wetland carbon fluxes in sites that are not monitored. To achieve this, we compare a range of models, from simple linear regression to advanced recurrent machine learning neural networks. Since the goal is to predict unseen sites, we emphasize cross-site predictability by validating and testing the models at sites not included in training. Doing so ensures predictions are applicable beyond the training sites and addresses challenges often associated with model generalizability (Meyer and Pebesma, 2022). This strategy serves several purposes:
 - 1. **Performance Contextualization**: Starting with the simplest type of model provides a baseline for performance and helps evaluate the advantage (or lack thereof) for using more complex models.
 - 2. **Practicality and Transparency**: Advanced models may offer better performance but often require significant effort to set up and may lack interpretability. By comparing models of varying complexity using the same input data, we assess whether the added complexity is justified.
 - 3. **Feature Evaluation**: Training with different combinations of relevant features helps us to understand which features are dominating control, and the limitations of the data in terms of predictive capacity.

2.1 Model targets

- The model targets two key variables: CO₂ (**FCO2**) and CH₄ (**FCH4**) surface emissions. Both variables follow a sign convention where positive values indicate emissions to the atmosphere (source) and negative values indicate sequestration (sink). Both variables are available at half-hourly resolution through the Ameriflux database.
- The models we developed all operate on a daily time scale, requiring target variables to be aggregated to the daily time scale. This approach assumes that sub-daily variations have a negligible non-linear contribution to longer time scales, an assumption supported by the dominant seasonal signal typically observed in flux data from these systems (Knox et al., 2021).
- 210 These target variables could then be used to calculate annual NECB (Net Ecosystem Carbon 211 Balance; gC m⁻² yr⁻¹) and annual wetland net atmospheric radiative effect (FCO₂e (CO₂-212 equivalent flux) qCO₂e m⁻² yr⁻¹). The global warming potential (GWP) of non-fossil CH₄ is 27.2 as 213 per the latest IPCC assessment (Lee et al., 2023). For this study, we neglect contributions of 214 lateral fluxes due to data limitations, and that lateral transport at these sites is assumed to be 215 negligible due to the limited outflow from these specific non-tidal wetland sites (Miller et al., 216 2008). FCO₂e is defined as annually averaged CO₂ and CH₄ emissions, adjusted for the global 217 warming potential (GWP) of each gas. A positive FCO₂e indicates that the ecosystem is 218 contributing positively to atmospheric warming, and vice versa. Here we consider CO₂ and CH₄ 219 emissions but neglect contributions from N2O due to data limitations and because N2O 220 emissions are considered negligible in Delta wetlands (Windham-Myers et al., 2018).

2.2 Region of interest

221

222

223

224

225

226

227

228

229

230

231

232

233

234

235

The Sacramento-San Joaquin Delta was selected for this study due to its high density of EC towers and extensive long-term data. We selected sites for model training and validation where data was collected for at least a decade to capture interannual variability. Hence three restored wetland sites, US-Myb (Matthes et al., 2016), US-Tw1 (Valach et al., 2016), and US-Tw4 (Eichelmann et al., 2016) are selected in this study. While data from two other sites (i.e., US-Sne and US-Tw5) are available, the lack of sufficient temporal coverage and, in the case of US-Sne, not fully established vegetation cover, makes them less representative of a stable ecosystem. Focusing on sites with over a decade of continuous data allows for capturing long-term dynamics more effectively and provides sufficient time for the wetlands to reach a stable state. The dataset encompasses 35 full site-years of observations across the three sites within the Delta (Novick et al., 2018) (Table 2, Figure 1), with detailed mapping data sourced from the Ecoatlas Database (Workgroup, 2019) which provides land use and vegetation surveys across wetlands in California.

Table 2: Model training sites

Site	Site Name	Water	Salinity	Years of	Start
Code		Туре		Data (Full)	Date
US-Myb	Mayberry Wetland	Non-Tidal	Fresh	13	2010
US-Tw1	Twitchell Wetland West Pond	Non-Tidal	Fresh	12	2011
US-Tw4	Twitchell Island East End Wetland	Non-Tidal	Fresh	10	2013

The sites are dominated by Tules (*Schoenoplectus*), Cattails (*Typha*), and invasive species such as *Phragmites*, which are perennial emergent plants well suited to wetland environments (López et al., 2016). The Delta itself is host to the largest estuarine system on the US Pacific coast, spanning approximately 3,000 km², and contains a diverse network of wetland systems. Historically, much of the area was drained and converted for agriculture (Laćan and Resh, 2016; Lund et al., 2010), but recent restoration efforts have reclaimed select portions of the landscape for environmental benefits.



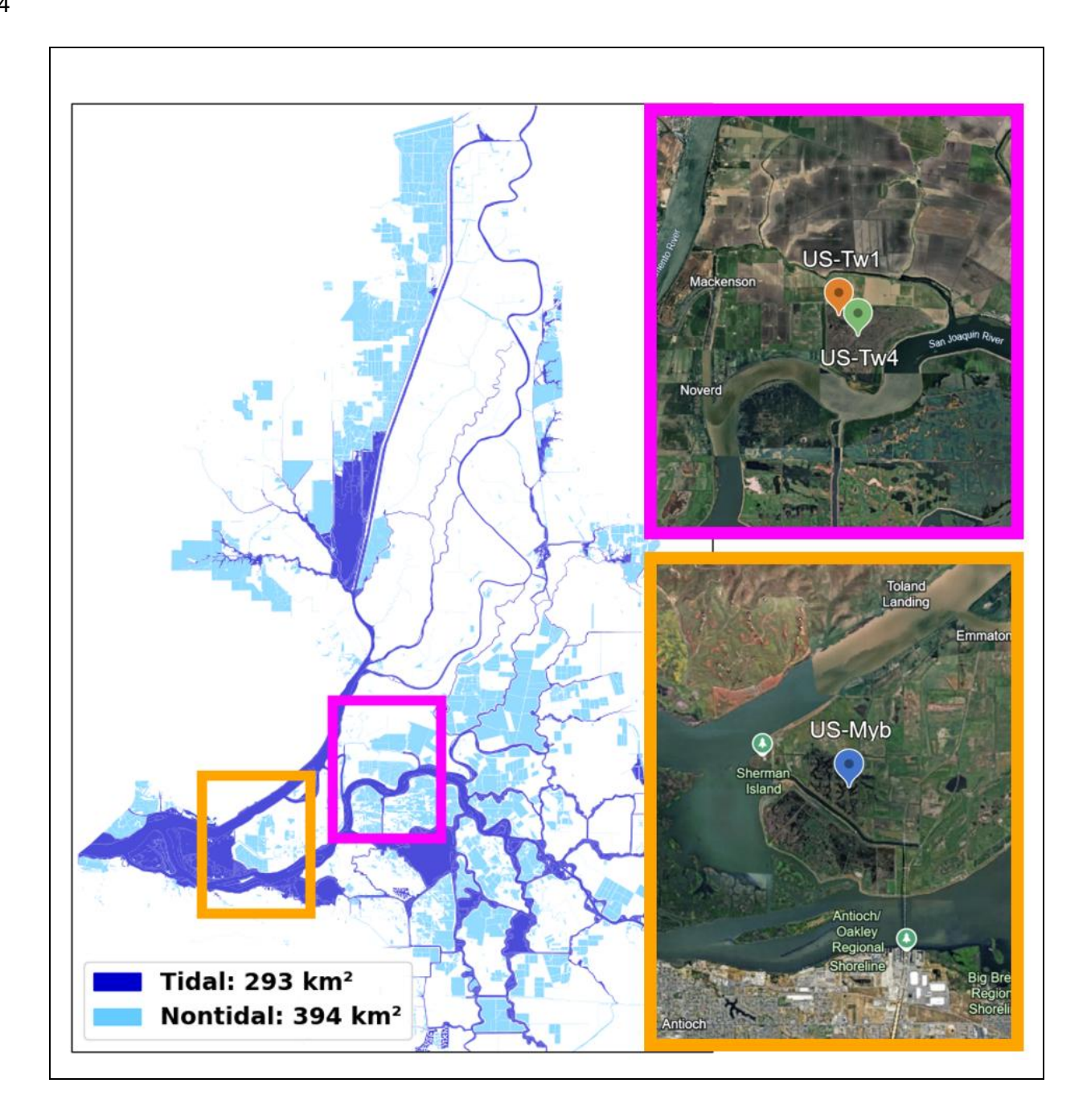


Figure 1: Map of the Sacramento-San Joaquin Delta's wetland system. The Eddy-covariance tower site locations outlined in Table 2 are shown in the red and purple boxes. Satellite image: © Google Earth, accessed 2025.

2.3 Model features

The application of this work focuses on upscaling carbon fluxes from similar wetlands at a regional scale. To achieve this, we aim to predict fluxes at unmonitored sites using widely available data that are expected to be key drivers of FCO2 and FCH4. Since site-level measurements from EC towers are not available at a larger spatial scale, we focus on ecosystem drivers that can be accessed across broader spatial extents.

The models utilize a comprehensive set of features from two readily accessible datasets: (i) the Western Land Data Assimilation System (WLDAS) (Erlingis et al., 2021) and (ii) Landsat surface-reflectance products (Landsat, 2020). A list of features can be found in Supplementary Table S3. Initially surface reflectance products were derived from MODIS (Justice et al., 2002), but we found better model performance with Landsat features. WLDAS provides hydrological and meteorological data at 1 km spatial and daily temporal resolution; we bilinearly interpolate these fields to each tower coordinate (no additional smoothing). Landsat offers 30 m pixels at a nominal 16-day revisit, although temporal resolution increases with time as more satellites are added; we average a 3 × 3 pixel window centred on the tower, linearly interpolate the series to daily resolution, and apply a centred 17-day running mean to improve data continuity.

2.4 Model suite

To evaluate ML model performance in calculating FCO2 and FCH4, we implemented a suite of seven models ranging from simple linear methods to more complex neural networks. These models have been used in various ecosystems to study fluxes and collectively represent a broad spectrum of methodological complexity. Table 3 summarizes the core characteristics and advantages of each approach.

Table 3: An overview of the models that are applied to wetland fluxes

Model Name	Category	Description	Key Strengths

Linear Regression	Regression	Fits a linear relationship between predictors and fluxes	Simple baseline, easily interpretable (Breiman, 2001)
Random Forest (Breiman, 2001)	Ensemble of Decision Trees	Aggregates multiple decision trees to enhance prediction stability	Robust to nonlinearity, reduces overfitting (Cortes, 1995)
Support Vector Machine (Cortes, 1995) (SVM)	Kernel-Based Method	Uses flexible kernels to find optimal separating hyperplanes	Effective in high dimensions, adaptable kernels (Ke et al., 2017)
LightGBM (Ke et al., 2017)	Gradient Boosting	Employs iterative boosting with efficient tree growth	Fast, memory- efficient, handles large datasets
XGBoost (Chen and Guestrin, 2016)	Gradient Boosting	Improves boosting with regularization and efficient computations	Manages outliers, handles sparse data well
LSTM Neural Network (Hochreiter, 1997)	Recurrent Neural Network	Captures temporal dependencies in sequential data inputs	Ideal for time- series, learns long-term patterns
GRU Neural Network (Chung et al., 2014)	Recurrent Neural Network	Similar to LSTM but streamlined with fewer parameters	Efficient temporal modeling, lower complexity

These models act to demonstrate a spectrum of model complexity and how that can be leveraged to improve flux prediction.

After performing simple grid searches we found that all models were largely insensitive to hyperparameter tuning, so we kept almost everything at the package defaults with some minor exceptions. Model hyper-parameter choices can be found in Brereton (2025).

2.5 Validation framework

To evaluate the models' ability to generalize across sites, we employed a Leave-One-Site-Out (LOSO) cross-validation strategy. In LOSO, we train the models on data from all but one site, and test the models on the excluded site. This approach is repeated for each site in the dataset

and then aggregated, ensuring that there are no spatio-temporal connections between the training and testing data. While few models are immune to overfitting, this approach minimizes the risk of doing so.

An integral part of our modeling approach is the strategic selection of input features to optimize the model's performance. We perform this selection by first selecting features that are expected to be important, guided by mechanistic considerations of wetland processes gained from fieldwork and insights from mechanistic models (Table S3). Since the total number of possible feature combinations is too large for an exhaustive search, we adopt a feed-forward selection (**FFS**) strategy. This method begins with a single feature and iteratively adds features that most improves the model's performance based on a chosen statistic. At each step, we evaluate the model's performance with each potential new feature and select the one that provides the greatest improvement. This process continues until adding additional features no longer significantly enhances the model's performance. By using this approach, we efficiently identify the most influential predictors without the computational burden of testing all possible combinations.

2.6. Validation

As suggested above, each model was trained using data from two wetland sites and then validated on the third. Although the number of sites was limited, each site offered over a decade of observations accumulated to a daily time step, ensuring exposure to a range of environmental conditions representative of the wetland type and regional climate. For each excluded site, the model's predictions were compared against measured FCO2 and FCH4 and we calculated R², Pearson's r, and RMSE for that site. We then pooled all held-out predictions from the three sites into one combined set and recomputed R² (as well as r and RMSE) on the full array to give an overall cross-validation score. This process was paired with the FFS method optimized to maximize R².

After selecting LSTM as the model of choice, it was retrained using all available data from the three sites for upscaling. The Sacramento-San Joaquin Delta contains roughly 700 km² of wetland area, including tidal and nontidal regions. The upscaling domain encompasses approximately 25 km² of nontidal wetlands in the region, dominated by vegetation types relevant to the training sites, specifically Tules, Cattails, and Phragmites. The assumption is that the training sites used in this study are representative of the broader conditions in the Delta, but we acknowledge that local variability in carbon dynamics, such as those caused by microclimates prevalent in the area, may not be fully captured during the ML model training. Improvements to the model might be achieved if additional site data covering a wider range of environmental conditions were incorporated. The feature data used to optimize the model were spatially interpolated onto the regional model grid and the model applied to yield flux estimations. Although relatively modest in spatial extent, these wetlands are of particular interest given their role in carbon sequestration and potential climate mitigation and as targets for conservation and restoration.

324

325

326

334

340

341

342

343

344

345

346

347

348

349

3. Results

3.1 Model Validation

for daily predictions are shown in Figure 2, demonstrating that nearly all machine learning models outperformed the linear regression baseline (R² = 0.64 for FCO2 and R² = 0.47 for FCH4). For FCO2, LSTM and GRU achieved the highest R² values (0.73 and 0.71, respectively), outperforming other methods. A similar result was found for FCH4, with LSTM and GRU both scoring R² of 0.53. These results suggest that deep learning models can provide tangible benefits over linear regression methods for upscaling flux predictions. The LSTM model

We tested six modeling techniques of varying complexities (Table 3). Model performance scores

333 was selected for upscaling in this study as it scored highest consistently, though other ML

models scored comparably, so we do not assert it as definitively the best model.

The feature selection process had access to 26 environmental features from WLDAS and 7 features derived from LANDSAT spectral bands (see table S3 for full details). These variables encompass a wide range of atmospheric, soil, and vegetation characteristics, such as precipitation, temperature, soil moisture, and spectral indices, key environmental drivers known to influence carbon and methane flux dynamics (Mitsch and Gosselink, 2015b).

The feature selection routine converged on variables that map directly onto the three main controls of wetland carbon cycling - vegetation productivity, surface energy-water balance, and microbial temperature sensitivity, see Table 4. For FCO2, the features selected were the Soil-Adjusted Vegetation Index (SAVI) and the upwards sensible heat flux, which are proxies for gross primary production and the surface energy water balance (Anderson et al., 2016; Huete, 1988). For FCH4, the features selected were canopy temperature, soil temperature and Greenness Difference Vegetation Index (GNDVI), which are proxies for short-term thermal forcing and vegetation water status, the anaerobic root-zone temperature that governs methanogenesis, and the supply of photosynthetically derived substrates for microbes, respectively (Bubier et al., 1993; Knox et al., 2021; Whiting and Chanton, 1993; Yvon-Durocher

350 et al., 2014).

351

352

Table 4: Feed-forward feature selection process.

Target Variable	Step	Chosen Feature	R²	RMSE	r
--------------------	------	----------------	----	------	---

FCO2	1	Soil-adjusted vegetation index (SAVI)	0.59	1.79	0.78
FCO2	2	(Upwards) sensible heat flux	0.73	1.46	0.86
FCH4	1	Canopy Temperature	0.48	0.054	0.70
FCH4	Soil temperature (10-40 cm)		0.52	0.052	0.73
FCH4	Normalized Difference Greenness Index (NDGI)		0.53	0.051	0.74

Figure 3 shows both FCO2 and FCH4 results, including time series and scatter plots comparing predictions to observations. Overall, the predicted values track the observations reasonably well. For FCO2, predictions tended to regress toward the mean, underestimating peak emissions at local maxima and overestimating at local minima, although reasonable interannual variability was observed. The ML models also displayed less interannual variability than the observations, common in machine learning approaches (Ouyang et al., 2023). For wetlands, this is likely due to limited subsurface process information included in the machine learning models. Still, the scatter plot shows strong performance for FCO2 (r = 0.86, $R^2 = 0.73$, RMSE = 1.46 gC-CO₂ m^{-2} day⁻¹), despite a noticeable spread around the 1:1 line.

FCH4 predictions exhibited similar behavior, with low interannual variability than the observations. At the US-Myb site, for example, observed FCH4 were initially high (aside from the first year, when vegetation cover had yet to be fully established) but declined over time, stabilizing at lower values. The ML models captured this shift to some extent, predicting higher fluxes early in the time series and then modulating to lower levels later on. However, predictions did not fully replicate the magnitude of the observed downward annual trend, introducing bias into the scatter plots at higher and lower extreme values. This phenomenon is known as regression to the mean, observed in similar machine learning studies (Ouyang et al., 2023). Consequently, the FCH4 model performance was weaker than the FCO2 model (R² = 0.53, r = 0.74, RMSE = 0.05 g C-CH4 m² day⁻¹), indicating that the processes controlling FCH4 in younger wetlands like US-Myb may require more detailed subsurface information (such as soil organic C, oxygen, or redox information) to be accurately modeled. Restored Delta wetlands are often net GHG sources for 1-3 years after flooding, before vegetation is fully established. Eddycovariance measurements show positive NEE of +201 ± 101 g C-CO₂ m⁻² yr⁻¹ and elevated

CH₄ emissions in the initial period, switching to sinks of between -400 to -700 g C-CO₂ m⁻² yr⁻¹ thereafter (Hemes et al., 2019). A larger synthesis found that this can persist decades in nontidal marshes because CH₄ radiative forcing outweighs CO₂ burial (Arias-Ortiz et al., 2021). Similar contrasts between 2 and 15-year-old wetlands (Knox et al., 2015).

382

383

384

385

386

387

388

389

390

391

392

393

394

395

396

397

398

399

400

378379

380

381

The annual bar plots presented in Figure 4 highlight the model's difficulty in capturing the interannual variability of carbon fluxes across the study sites. While the average FCO2 and FCH4 predictions are generally aligned with observed average values with small overall mean bias, the model struggles to reproduce the observed year-to-year variability. Although direct subsurface measurements are available at certain sites, at the regional scale their limited spatial and temporal coverage currently limits integration into models designed for regional upscaling over inter-annual timescale. For example, while spatial maps of wetland soil organic carbon exist (Uhran et al., 2022), using only three sites for training purposes would provide just three corresponding data points, limiting model training. The LOSO validation approach revealed that deep learning models, particularly LSTM and GRU, consistently outperformed traditional linear regression and other machine learning methods for both FCO2 and FCH4 predictions. While nonlinear models demonstrated clear advantages, the magnitude of improvement was relatively modest, reflecting the inherent challenges of capturing site-specific inter-annual dynamics of wetland emissions. To improve model performance, additional techniques such as feature transformations or attention mechanisms could be implemented. However, the primary goal of this model suite is to ensure reproducible results with 'off-the-shelf' models, which serves as a foundation for more advanced, nuanced approaches.

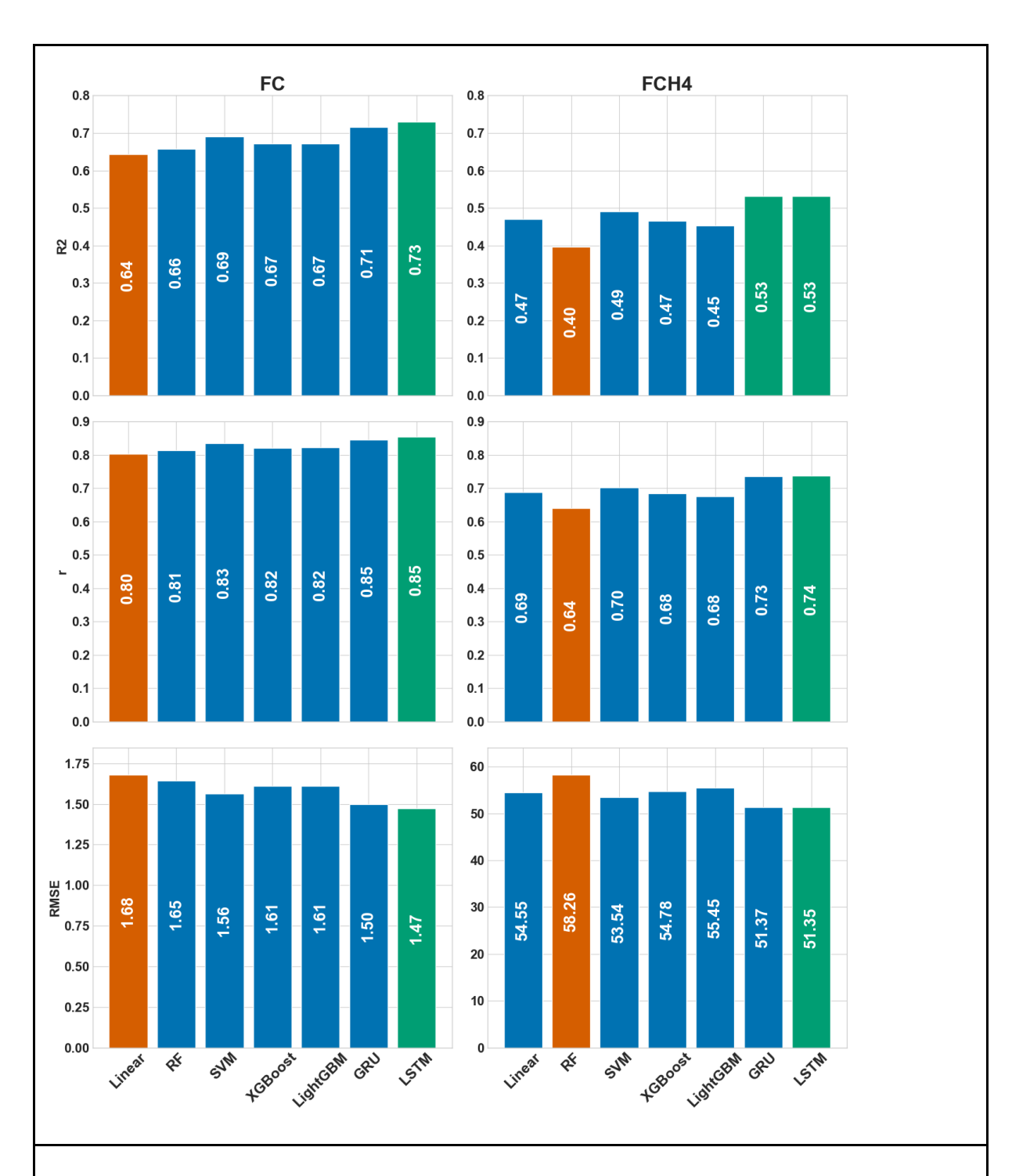


Figure 2: Bar plot showing best model performance for each type of machine learning model based on R² score (though other metrics are in agreement, see Pearson r correlation and RMSE).

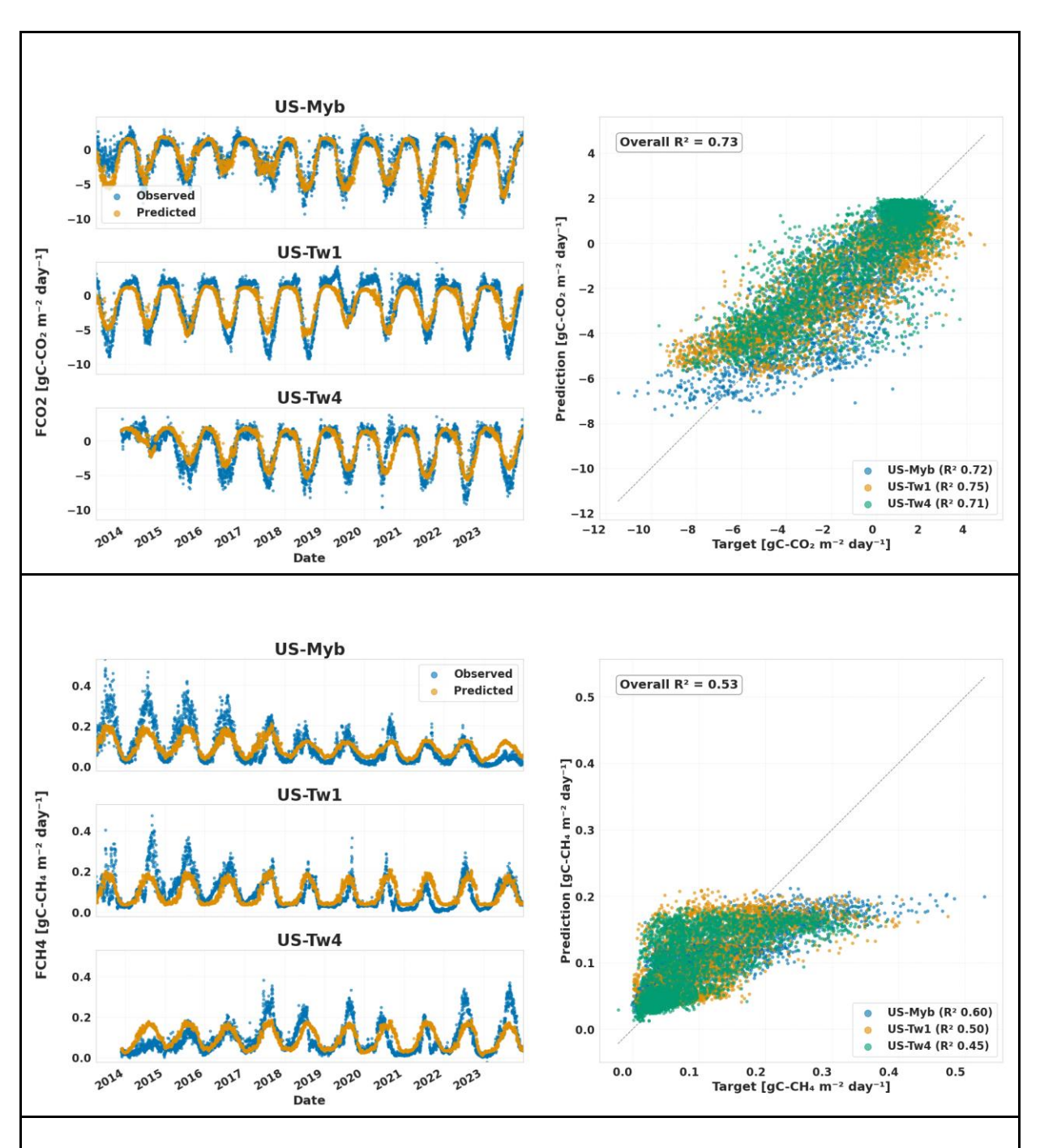


Figure 3: Time-series plots (left) of observed (blue) and predicted (orange) FCO2 and FCH4 fluxes for US-Myb, US-Tw1, and US-Tw4. The scatter plot (right) compares observed vs. predicted values across all sites, with a 1:1 reference line with overall and site-only performance metrics (R²).

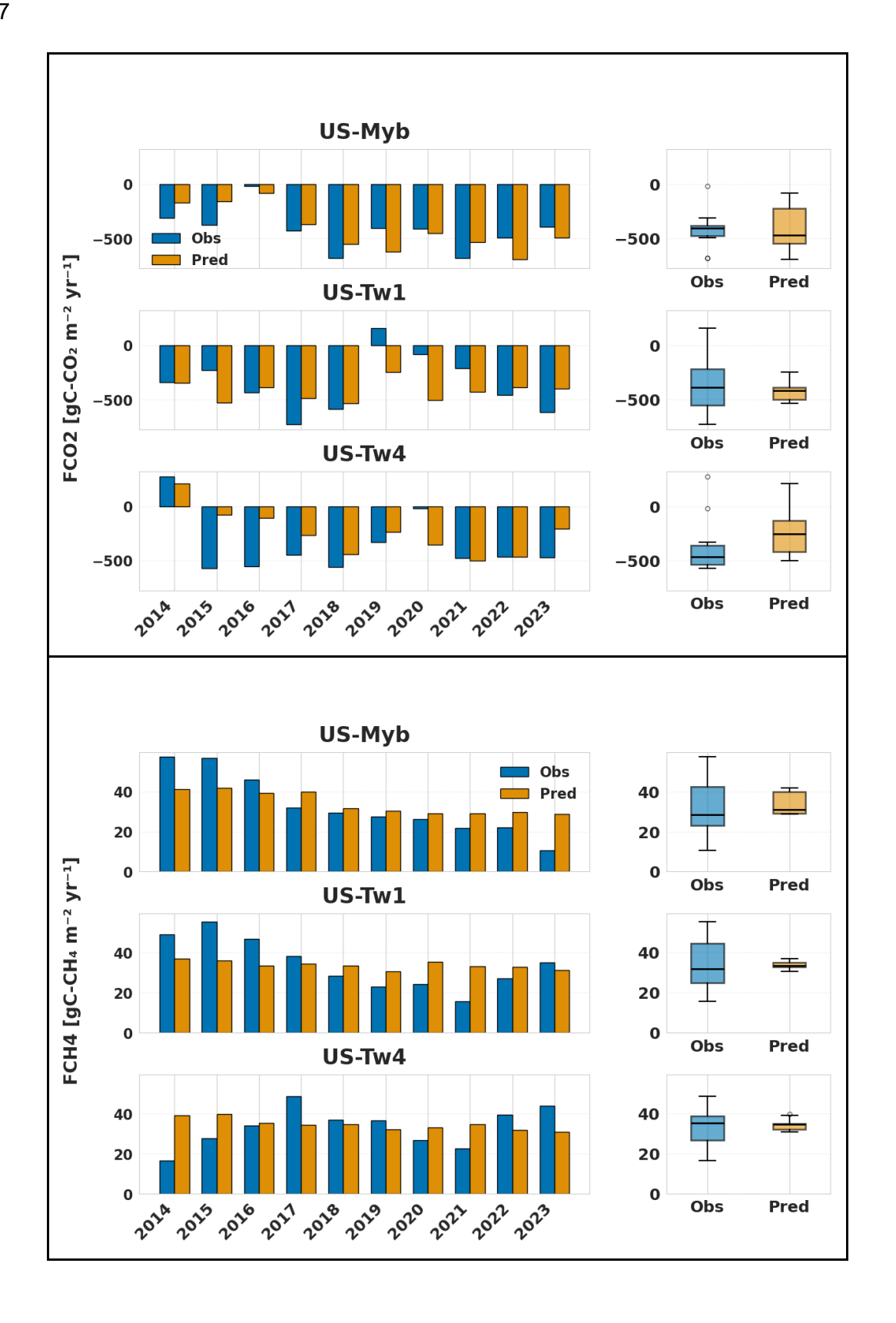


Figure 4: Annual Observed and Predicted FCO2 and FCH4 Across Three Wetland Sites. Aggregated statistics for all sites are as follows: For **FCO2**, the Mean Absolute Error (MAE) is **176 gC m⁻² yr⁻¹** and the Mean Bias Error (MBE) is **17 gC m⁻² yr⁻¹**. For **FCH4**, MAE is **9 gC-CH₄ m⁻² yr⁻¹** and the MBE is **1gC-CH₄ m⁻² yr⁻¹**.

408

409

410

411

412

413

414

415

416

417

418

419

420

421

422

423

424

425

426

427

428

429

430

431

432

3.2. Model Application: Upscaling Upscaling was repeated 10 times for 10 separately trained ML models using the same data, and the ensemble mean is the value reported, as training includes stochasticity. Figure 5 displays spatial maps of annual flux estimates of Net Ecosystem Carbon Balance (NECB), and the CO2 equivalent flux rate (FCO2e) in the study domain, including zoom-in subplots highlighting areas with more data. The results show that carbon sequestration, indicated by negative NECB (green) values, are typically dominant throughout the domain, although the northern regions show more carbon sources. In contrast, the FCO2e distribution shows variability across the region, with sources and sinks found CO₂e sink throughout. Figure S1 plots the coefficient of variation (CV = σ/μ) of the inter-model ensemble for both NECB and FCO₂e. Higher CV indicates locations where environmental conditions are poorly represented in the training data - effectively a proxy to determine model confidence. Across the study domain the vast majority of pixels show low dispersion: ≈ 85 % of the mapped area has a CV < 0.5 for NECB, and 69 % falls below that same threshold for FCO₂e. Figure 6 shows averaged fluxes in the upscaling domain over the full study period. The results highlight the Delta as an overall carbon sink, with NECB averaging approximately -450 gC m⁻² yr⁻¹, indicating persistent sequestration across multiple years. CH₄ fluxes average 31 gC-CH₄ m⁻² yr⁻¹, and shows little spatial variability. Values are consistent with those previously reported in the region (Arias-Ortiz et al., 2021). Integrating these fluxes into a CO₂-equivalent metric, this regional wetland system remains a net sink of CO₂e, with approximately 600 gCO₂e m⁻² yr⁻¹

sequestered on average in the upscaling domain, with an increasing trend with time.

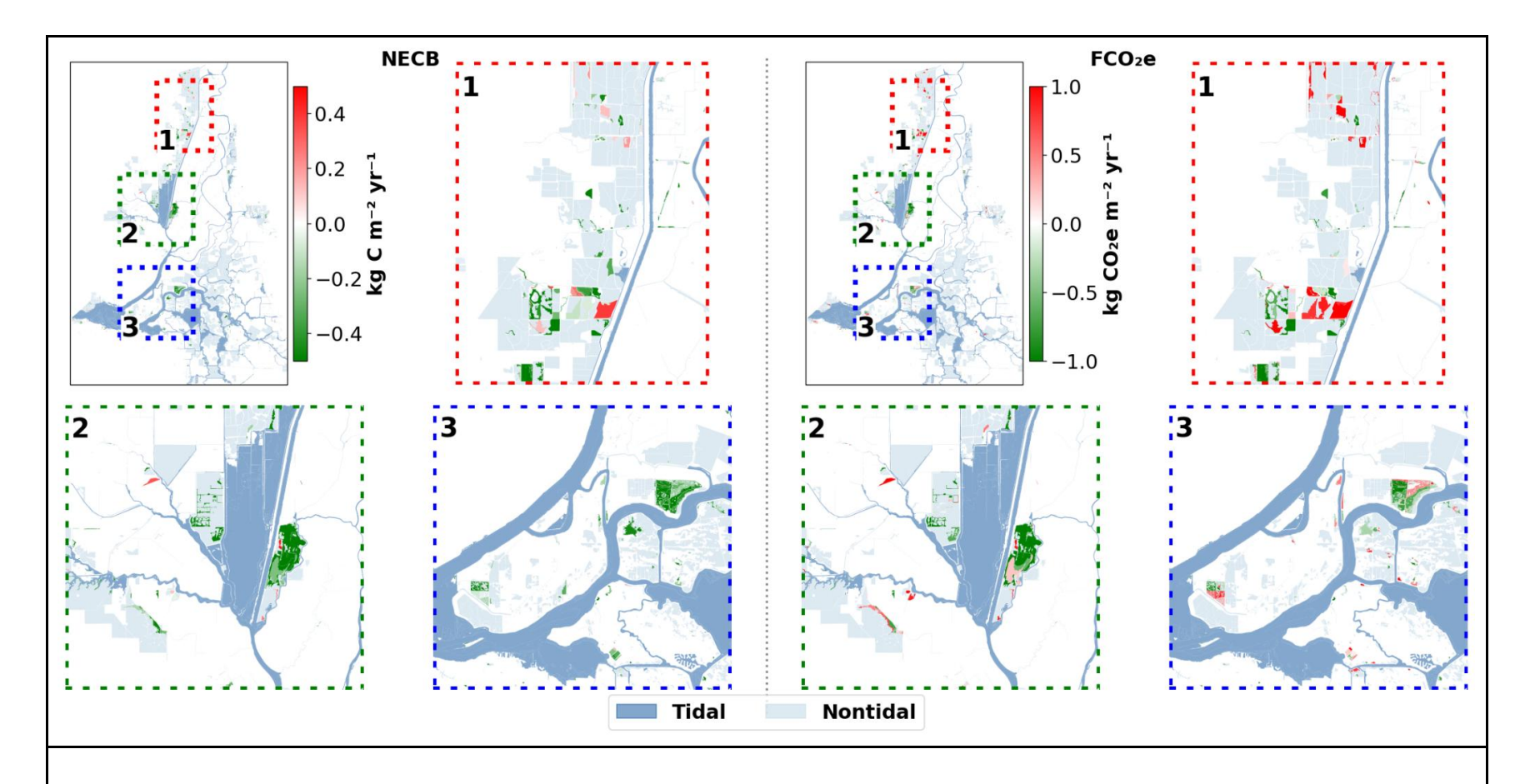


Figure 5: Mean annual Net Ecosystem Carbon Balance (NECB, left) and CO₂-equivalent radiative forcing (FCO₂e, right) averaged over all model years. Main maps show the Delta area; dashed rectangles (1 - 3) correspond to zoom-in panels. Tidal wetlands are shaded dark blue, non-tidal light blue. Positive values (red) indicate net carbon loss; negative values (green) net uptake. See Figure 1 for reference to training sites.



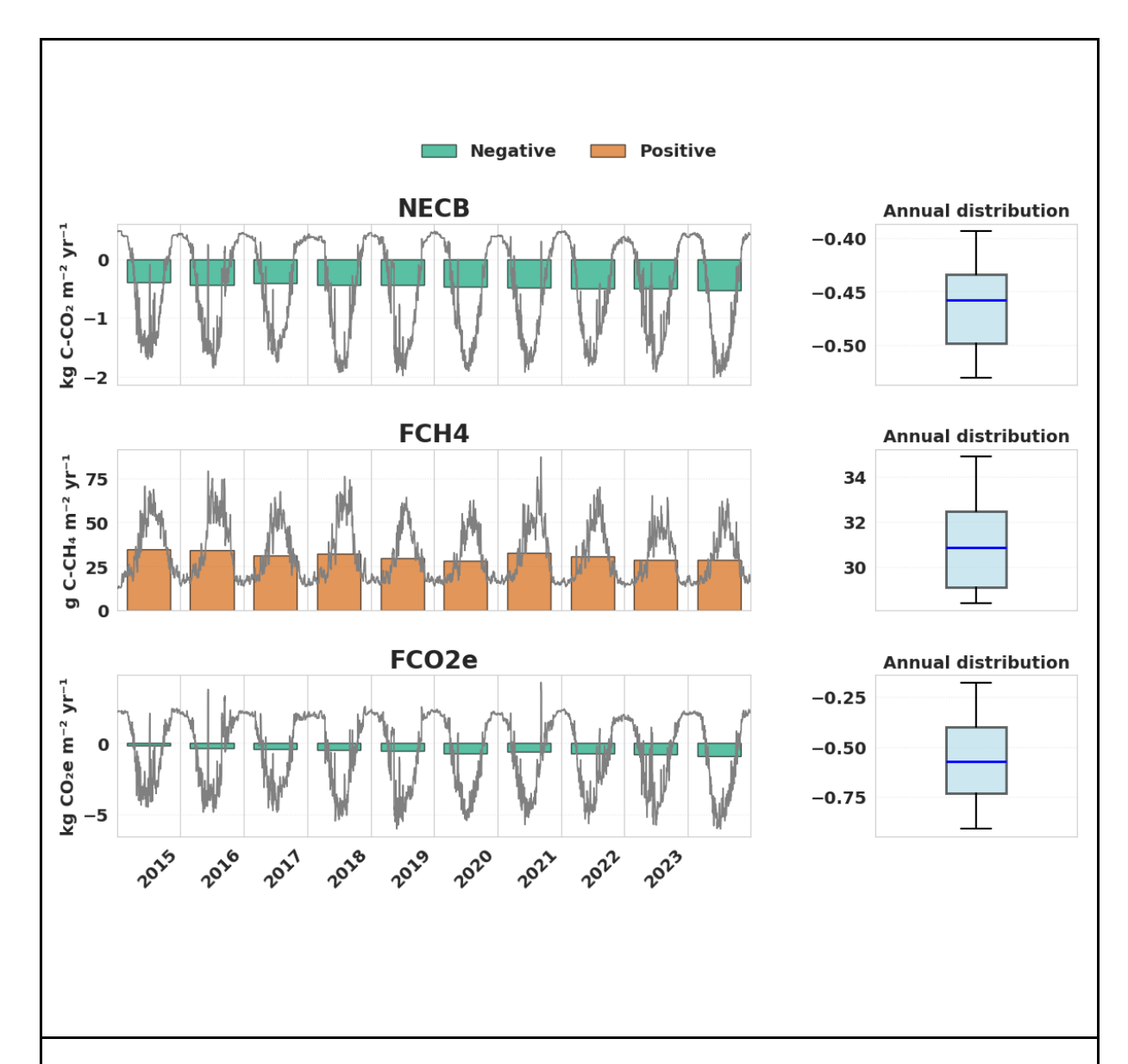


Figure 6: Bar plots and box plots of annual NECB, FCH4, and FCO₂e fluxes, which have been spatially integrated over the study region, a total of 25 km² total land area vegetated primarily by Tules, but also Cattails and Phragmites. The left column shows annual fluxes for each year, with negative fluxes in green and positive fluxes in orange. Daily fluxes, aggregated to annual totals, are overlaid as grey lines. The right column shows box plots summarizing the distribution of annual fluxes, highlighting the range, median (blue line), and

spread of values. Each row represents a different flux variable: (a) NECB, (b) FCH4, and (c) FCO₂e.

4. Discussion

- 440 This study demonstrates the development and evaluation of a data-driven framework to upscale
- 441 terrestrial CO₂ and CH₄ flux estimates for non-tidal wetlands in the Sacramento-San Joaquin
- 442 Delta. By systematically comparing models of varying complexity, including linear regression,
- 443 ensemble methods, gradient boosting algorithms, and recurrent neural networks (RNNs), we
- 444 presented a transparent assessment of model performance. The goals were to identify the
- 445 model that best predicts CO₂ and CH₄ fluxes and critically appraise whether incremental
- 446 complexity is justified by improvements in predictive capacity. Relevant cited works have
- 447 included many different machine learning approaches for predicting emissions. This work aims
- 448 to unify modelling efforts by establishing a standard framework for developing robust data-
- 449 driven models, particularly for upscaling purposes.
- 450 Our results indicate that non-linear and more advanced models generally outperformed simple
- 451 linear regression approaches. Among all tested models, the Long Short-Term Memory (LSTM)
- and Gated Recurrent Unit (GRU) neural networks provided the highest overall skill in predicting 452
- both CO₂ and CH₄ fluxes at daily timescales. This improvement was marginal but consistent. 453
- 454 supporting the notion that time-series models, which inherently capture temporal dependencies
- 455 and non-linearities, can provide tangible benefits over linear methods and traditional machine
- 456 learning algorithms.
- 457 However, while these deep learning models performed best, the performance gains were not as
- 458 large as might be expected given their significantly higher complexity and computational
- 459 demands. Similar outcomes have been noted in other ecological modeling applications, where
- 460 advanced machine learning methods yield improvements that are statistically significant yet
- 461 modest in terms of performance gains relative to linear models (Oh et al., 2022; Wood, 2022).
- 462 The deep learning models provided reasonable estimates of daily fluxes but struggled to
- 463 replicate the full range of interannual variability observed in the field measurements, which is a
- 464 common issue for data-driven models in this field (Nelson et al., 2024). This limited ability to
- 465 capture long-term trends and extremes mirrors common challenges in machine learning-based
- modeling, where the absence of explicit mechanistic understanding limits extrapolation beyond
- 466
- 467 the conditions represented in the training data. The difficulty in reproducing interannual
- 468 fluctuations was particularly evident for CH₄ fluxes, an outcome consistent with the high spatial
- 469 and temporal complexity of CH₄ cycling in wetland environments and the limited availability of
- 470 subsurface parameters (e.g., oxygen concentration, redox conditions, substrate availability) that
- 471 drive CH₄ production. This may not be surprising as the number of annual cycles available in
- 472 the training set was only 35 years.

473 The observed regression to the mean and the reduced dynamic range in model predictions may 474 reflect insufficient representation of key environmental drivers in the feature set or inadequate 475 temporal coverage and variability in the training data. While publicly available datasets such as 476 WLDAS and LANDSAT were effective at providing spatially and temporally comprehensive 477 inputs, the lack of direct subsurface and soil biogeochemical measurements likely limited the 478 model's ability to capture critical internal processes that are likely causing the observed 479 differences between years. Although the feed-forward selection process for the model features 480 had access to an extensive pool of relevant features, results indicated that only a small subset 481 of features was necessary to maximise performance. This suggests that, while there are many 482 features that control CO₂ and CH₄, their contribution to predictive accuracy may be redundant or 483 captured indirectly by other variables. The exclusion of particular features, such as the water 484 table depth for FCH4, illustrates the trade-off between mechanistic intuition and data-driven 485 optimization. Strong correlations between features with limited independent variability can lead 486 to features being left out that would typically be considered ecologically relevant.

487 The feed-forward selection converges on a compact set of features that are mechanistically 488 expected to drive CO2 and CH4 gas exchange in natural wetlands, adding qualitative 489 confidence to the model; see Table 4 for the list of features selected. For FCO2; the model 490 selected SAVI (Soil-Adjusted Vegetation Index), which represents vegetation state and 491 photosynthetic capacity, and upward sensible heat flux (Qh), which is related to the rate of 492 evapotranspiration. For FCH4, canopy temperature and GNDVI (Greenness index) indicate 493 plant activity and substrate supply via plant-mediated transport, while 10-40 cm soil temperature 494 reflects anaerobic microbial production (methanogenesis) in the root zone.

After applying the chosen model (LSTM) to calculate CO₂ and CH₄ fluxes, we estimated NECB and CO₂-equivalent fluxes for similar wetland settings across the Delta region (Figure 5). The results show spatial heterogeneity and pinpoint regions that act as stronger net carbon sinks, as well as areas where CH₄ emissions may offset climate benefits of net carbon sequestration. Such insights support targeted conservation and restoration strategies aimed at maximizing net carbon sequestration benefits, facilitating ongoing efforts to restore and manage wetlands to contribute to net-zero emission goals.

A key advantage of the chosen approach is its reliance on readily available, open-source data streams and standard computational resources. The framework can be deployed efficiently without specialized hardware, making it accessible to resource-limited organizations, practitioners, and researchers.

The primary objectives of this study were to identify a suitable model, contextualize model performance by comparing to a baseline linear regression, and highlight trade-offs between complexity, interpretability, and accuracy. By explicitly testing multiple models ranging from simple linear regressions to advanced recurrent neural networks, we demonstrated that complexity alone does not guarantee a substantial increase in predictive power. Instead, complexity should be adopted judiciously, based on the magnitude of performance gains, the cost of model implementation, and the level of interpretability.

495

496

497

498

499

500

501

502

503

504

505

506

507

508

509

510

511

We suggest that future modeling efforts should focus on deriving mechanistically relevant predictors (Ouyang et al., 2023), and incorporating hybrid modeling approaches (Yao et al., 2023) that combine the strengths of process-based and machine learning methods. Attention mechanisms (Yuan et al., 2022), advanced architectures (e.g., Transformers (Vaswani, 2017)), or physics-informed machine learning (Raissi et al., 2019) may also help address model performance limitations.

519

520

5. Conclusions

521 522

523

524

525

526

527

528

529

530

531

532

This study provides a transparent, methodical demonstration of an artificial intelligence approach to modeling wetland carbon dioxide (CO₂) and methane (CH₄) emissions, using a suite of "off-the-shelf" tools and establishing a standardized benchmarking protocol for model performance evaluation. In the study region (the Sacramento–San Joaquin Delta), inter-model comparisons revealed modest but appreciable performance differences when comparing advanced models with a linear regression baseline. While there are tangible benefits to employing machine learning for these purposes, it is likely that the gap between simpler models and more sophisticated models will widen as data quantity and quality continues to increase. Ultimately, this study lays the groundwork for regional scale model benchmark testing, facilitating the development of more advanced modeling approaches that can guide wetland management, restoration planning, and climate mitigation strategies.

533

534

539

Code and data availability

- 535 The current version of the **RCCAT model** is available on GitHub at
- 536 https://github.com/ashbre2/RCCAT under the MIT License. The exact version of the model
- used to produce the results presented in this paper has been archived on Zenodo (Brereton,
- 538 2025)

Author contributions

- Ashley developed the model, performed the analysis, and led the writing of the manuscript.
- Zelalem, Bhavna, Adina, William and Kunxiaojia contributed to model development and
- 542 provided expertise in carbon flux modeling. Qian contributed expertise in machine learning
- 543 methods. Tyler provided domain-specific knowledge of the region of interest. Yu and Yi
- 544 contributed expertise in hydrological processes. All co-authors reviewed, provided input on the
- 545 manuscript drafts, and approved the final version.

546

- Abril, G. and Iversen, N.: Methane dynamics in a shallow non-tidal estuary (Randers Fjord,
- 549 Denmark), Mar. Ecol. Prog. Ser., 230, 171–181, 2002.
- Anderson, F. E., Bergamaschi, B., Sturtevant, C., Knox, S., Hastings, L., Windham-Myers, L.,
- Detto, M., Hestir, E. L., Drexler, J., Miller, R. L., Matthes, J. H., Verfaillie, J., Baldocchi, D.,
- 552 Snyder, R. L., and Fujii, R.: Variation of energy and carbon fluxes from a restored temperate
- freshwater wetland and implications for carbon market verification protocols, J. Geophys. Res.
- 554 Biogeosciences, 121, 777–795, https://doi.org/10.1002/2015JG003083, 2016.
- Anderson, M., Gao, F., Knipper, K., Hain, C., Dulaney, W., Baldocchi, D., Eichelmann, E.,
- Hemes, K., Yang, Y., and Medellin-Azuara, J.: Field-scale assessment of land and water use
- 557 change over the California Delta using remote sensing, Remote Sens., 10, 889, 2018.
- Arias-Ortiz, A., Oikawa, P. Y., Carlin, J., Masqué, P., Shahan, J., Kanneg, S., Paytan, A., and
- 559 Baldocchi, D. D.: Tidal and Nontidal Marsh Restoration: A Trade-Off Between Carbon
- Sequestration, Methane Emissions, and Soil Accretion, J. Geophys. Res. Biogeosciences, 126,
- e2021JG006573, https://doi.org/10.1029/2021JG006573, 2021.
- Arora, B., Wainwright, H. M., Dwivedi, D., Vaughn, L. J., Curtis, J. B., Torn, M. S., Dafflon, B.,
- and Hubbard, S. S.: Evaluating temporal controls on greenhouse gas (GHG) fluxes in an Arctic
- tundra environment: An entropy-based approach, Sci. Total Environ., 649, 284–299, 2019.
- Arora, B., Briggs, M. A., Zarnetske, J. P., Stegen, J., Gomez-Velez, J. D., Dwivedi, D., and
- 566 Steefel, C.: Hot Spots and Hot Moments in the Critical Zone: Identification of and Incorporation
- into Reactive Transport Models, in: Biogeochemistry of the Critical Zone, edited by: Wymore, A.
- 568 S., Yang, W. H., Silver, W. L., McDowell, W. H., and Chorover, J., Springer International
- 569 Publishing, Cham, 9–47, https://doi.org/10.1007/978-3-030-95921-0 2, 2022.
- 570 Ashley: Regional Carbon Climate Analytics Tool (RCCAT), 2025.
- Aubinet, M., Vesala, T., and Papale, D.: Eddy covariance: a practical guide to measurement and
- 572 data analysis, Springer Science & Business Media, 2012.
- Baldocchi, D., Falge, E., Gu, L., Olson, R., Hollinger, D., Running, S., Anthoni, P., Bernhofer, C.,
- 574 Davis, K., and Evans, R.: FLUXNET: A new tool to study the temporal and spatial variability of
- ecosystem-scale carbon dioxide, water vapor, and energy flux densities, Bull. Am. Meteorol.
- 576 Soc., 82, 2415–2434, 2001.
- 577 Bergmeir, C. and Benítez, J. M.: On the use of cross-validation for time series predictor
- 578 evaluation, Inf. Sci., 191, 192–213, 2012.
- 579 Bernal, B. and Mitsch, W. J.: Comparing carbon sequestration in temperate freshwater wetland
- 580 communities, Glob. Change Biol., 18, 1636–1647, https://doi.org/10.1111/j.1365-
- 581 2486.2011.02619.x, 2012.
- Bodesheim, P., Jung, M., Gans, F., Mahecha, M. D., and Reichstein, M.: Upscaled diurnal
- 583 cycles of land-atmosphere fluxes: a new global half-hourly data product, Earth Syst. Sci. Data,
- 584 10, 1327–1365, 2018.
- 585 Breiman, L.: Random Forests, Mach. Learn., 45, 5–32,
- 586 https://doi.org/10.1023/A:1010933404324, 2001.

- 587 Brereton, A. Regional Carbon Climate Analytics Tool (RCCAT), version 1.0.0, Zenodo,
- 588 https://doi.org/10.5281/zenodo.14933820, 2025.
- Brix, H., Sorrell, B. K., and Lorenzen, B.: Are Phragmites-dominated wetlands a net source or
- 590 net sink of greenhouse gases?, Aquat. Bot., 69, 313–324, 2001.
- Bubier, J., Costello, A., Moore, T. R., Roulet, N. T., and Savage, K.: Microtopography and
- methane flux in boreal peatlands, northern Ontario, Canada, Can. J. Bot., 71, 1056–1063,
- 593 https://doi.org/10.1139/b93-122, 1993.
- 594 Carnell, P. E., Windecker, S. M., Brenker, M., Baldock, J., Masque, P., Brunt, K., and
- 595 Macreadie, P. I.: Carbon stocks, sequestration, and emissions of wetlands in south eastern
- 596 Australia, Glob. Change Biol., 24, 4173–4184, https://doi.org/10.1111/gcb.14319, 2018.
- 597 Chen, T. and Guestrin, C.: XGBoost: A Scalable Tree Boosting System, in: Proceedings of the
- 598 22nd ACM SIGKDD International Conference on Knowledge Discovery and Data Mining, KDD
- in 16: The 22nd ACM SIGKDD International Conference on Knowledge Discovery and Data
- 600 Mining, San Francisco California USA, 785–794, https://doi.org/10.1145/2939672.2939785,
- 601 2016.
- 602 Chu, H., Luo, X., Ouyang, Z., Chan, W. S., Dengel, S., Biraud, S. C., Torn, M. S., Metzger, S.,
- Kumar, J., and Arain, M. A.: Representativeness of Eddy-Covariance flux footprints for areas
- surrounding AmeriFlux sites, Agric. For. Meteorol., 301, 108350, 2021.
- 605 Chung, J., Gulcehre, C., Cho, K., and Bengio, Y.: Empirical Evaluation of Gated Recurrent
- Neural Networks on Sequence Modeling, https://doi.org/10.48550/arXiv.1412.3555, 11
- 607 December 2014.
- 608 Ciais, P., Borges, A. V., Abril, G., Meybeck, M., Folberth, G., Hauglustaine, D., and Janssens, I.
- A.: The impact of lateral carbon fluxes on the European carbon balance, Biogeosciences, 5,
- 610 1259–1271, 2008.
- 611 Cortes, C.: Support-Vector Networks, Mach. Learn., 1995.
- 612 Costanza, R., De Groot, R., Sutton, P., Van der Ploeg, S., Anderson, S. J., Kubiszewski, I.,
- Farber, S., and Turner, R. K.: Changes in the global value of ecosystem services, Glob.
- 614 Environ. Change, 26, 152–158, 2014.
- DeLaune, R. D. and Pezeshki, S. R.: The role of soil organic carbon in maintaining surface
- elevation in rapidly subsiding US Gulf of Mexico coastal marshes, Water Air Soil Pollut. Focus,
- 617 3, 167–179, 2003.
- 618 Ding, H.: Establishing a soil carbon flux monitoring system based on support vector machine
- and XGBoost, Soft Comput., 28, 4551–4574, 2024.
- 620 Eichelmann, E., Shortt, R., Knox, S., Sanchez, C. R., Valach, A., Sturtevant, C., Szutu, D.,
- 621 Verfaillie, J., and Baldocchi, D.: AmeriFlux AmeriFlux US-Tw4 Twitchell East End Wetland,
- 622 Lawrence Berkeley National Laboratory (LBNL), Berkeley, CA (United States ..., 2016.
- 623 Erlingis, J. M., Rodell, M., Peters-Lidard, C. D., Li, B., Kumar, S. V., Famiglietti, J. S., Granger,
- S. L., Hurley, J. V., Liu, P., and Mocko, D. M.: A High-Resolution Land Data Assimilation

- 625 System Optimized for the Western United States, JAWRA J. Am. Water Resour. Assoc., 57,
- 626 692–710, https://doi.org/10.1111/1752-1688.12910, 2021.
- 627 Grande, E., Seybold, E. C., Tatariw, C., Visser, A., Braswell, A., Arora, B., Birgand, F., Haskins,
- 628 J., and Zimmer, M.: Seasonal and tidal variations in hydrologic inputs drive salt marsh
- porewater nitrate dynamics, Hydrol. Process., 37, e14951, https://doi.org/10.1002/hyp.14951,
- 630 2023.
- Grant, R. F. and Roulet, N. T.: Methane efflux from boreal wetlands: Theory and testing of the
- ecosystem model Ecosys with chamber and tower flux measurements, Glob. Biogeochem.
- 633 Cycles, 16, https://doi.org/10.1029/2001GB001702, 2002.
- Grant, R. F., Mekonnen, Z. A., Riley, W. J., Arora, B., and Torn, M. S.: 2. Microtopography
- determines how CO2 and CH4 exchange responds to changes in temperature and precipitation
- at an Arctic polygonal tundra site: mathematical modelling with ecosys, J Geophys Res
- 637 Biogeosci, 122, 3174–3187, 2017.
- Harrison, R. B., Footen, P. W., and Strahm, B. D.: Deep soil horizons: contribution and
- 639 importance to soil carbon pools and in assessing whole-ecosystem response to management
- and global change, For. Sci., 57, 67–76, 2011.
- Hastie, T.: The elements of statistical learning: data mining, inference, and prediction, 2009.
- Hemes, K. S., Chamberlain, S. D., Eichelmann, E., Anthony, T., Valach, A., Kasak, K., Szutu,
- D., Verfaillie, J., Silver, W. L., and Baldocchi, D. D.: Assessing the carbon and climate benefit of
- restoring degraded agricultural peat soils to managed wetlands, Agric. For. Meteorol., 268, 202-
- 645 214, 2019.
- Hill, T., Chocholek, M., and Clement, R.: The case for increasing the statistical power of eddy
- covariance ecosystem studies: why, where and how?, Glob. Change Biol., 23, 2154–2165,
- 648 https://doi.org/10.1111/gcb.13547, 2017.
- Hochreiter, S.: Long Short-term Memory, Neural Comput. MIT-Press, 1997.
- Huete, A. R.: A soil-adjusted vegetation index (SAVI), Remote Sens. Environ., 25, 295–309,
- 651 1988.
- Justice, C. O., Townshend, J. R. G., Vermote, E. F., Masuoka, E., Wolfe, R. E., Saleous, N.,
- Roy, D. P., and Morisette, J. T.: An overview of MODIS Land data processing and product
- 654 status, Remote Sens. Environ., 83, 3–15, 2002.
- 655 Kaufman, S., Rosset, S., Perlich, C., and Stitelman, O.: Leakage in data mining: Formulation,
- detection, and avoidance, ACM Trans. Knowl. Discov. Data, 6, 1–21,
- 657 https://doi.org/10.1145/2382577.2382579, 2012.
- 658 Ke, G., Meng, Q., Finley, T., Wang, T., Chen, W., Ma, W., Ye, Q., and Liu, T.-Y.: Lightgbm: A
- 659 highly efficient gradient boosting decision tree, Adv. Neural Inf. Process. Syst., 30, 2017.
- de Klein, J. J. and van der Werf, A. K.: Balancing carbon sequestration and GHG emissions in a
- 661 constructed wetland, Ecol. Eng., 66, 36–42, 2014.

- Knox, S. H., Sturtevant, C., Matthes, J. H., Koteen, L., Verfaillie, J., and Baldocchi, D.:
- Agricultural peatland restoration: effects of land-use change on greenhouse gas (CO₂ and CH₄)
- fluxes in the Sacramento-San Joaquin Delta, Glob. Change Biol., 21, 750–765,
- 665 https://doi.org/10.1111/gcb.12745, 2015.
- 666 Knox, S. H., Dronova, I., Sturtevant, C., Oikawa, P. Y., Matthes, J. H., Verfaillie, J., and
- Baldocchi, D.: Using digital camera and Landsat imagery with eddy covariance data to model
- gross primary production in restored wetlands, Agric. For. Meteorol., 237, 233–245, 2017.
- Knox, S. H., Bansal, S., McNicol, G., Schafer, K., Sturtevant, C., Ueyama, M., Valach, A. C.,
- Baldocchi, D., Delwiche, K., Desai, A. R., Euskirchen, E., Liu, J., Lohila, A., Malhotra, A.,
- Melling, L., Riley, W., Runkle, B. R. K., Turner, J., Vargas, R., Zhu, Q., Alto, T., Fluet-Chouinard,
- E., Goeckede, M., Melton, J. R., Sonnentag, O., Vesala, T., Ward, E., Zhang, Z., Feron, S.,
- Ouyang, Z., Alekseychik, P., Aurela, M., Bohrer, G., Campbell, D. I., Chen, J., Chu, H.,
- Dalmagro, H. J., Goodrich, J. P., Gottschalk, P., Hirano, T., Iwata, H., Jurasinski, G., Kang, M.,
- Koebsch, F., Mammarella, I., Nilsson, M. B., Ono, K., Peichl, M., Peltola, O., Ryu, Y., Sachs, T.,
- Sakabe, A., Sparks, J. P., Tuittila, E., Vourlitis, G. L., Wong, G. X., Windham-Myers, L., Poulter,
- B., and Jackson, R. B.: Identifying dominant environmental predictors of freshwater wetland
- methane fluxes across diurnal to seasonal time scales, Glob. Change Biol., 27, 3582–3604,
- 679 https://doi.org/10.1111/gcb.15661, 2021.
- 680 Kumar, A., Bhatia, A., Fagodiya, R. K., Malyan, S. K., and Meena, B. L.: Eddy covariance flux
- tower: A promising technique for greenhouse gases measurement, Adv Plants Agric Res, 7,
- 682 337–340, 2017.
- Laćan, I. and Resh, V. H.: A case study in integrated management: Sacramento-San Joaquin
- 684 Rivers and Delta of California, USA, Ecohydrol. Hydrobiol., 16, 215–228, 2016.
- 685 Landsat, U.: Landsat 8-9Operational Land Imager (OLI)-Thermal Infrared Sensor (TIRS)
- 686 Collection 2 Level 2 (L2) Data Format Control Book (DFCB), U. S. Geol. Surv. Rest. VA USA,
- 687 78, 2020.
- Lee, H., Calvin, K., Dasgupta, D., Krinner, G., Mukherji, A., Thorne, P., Trisos, C., Romero, J.,
- 689 Aldunce, P., and Barrett, K.: Climate change 2023: synthesis report. Contribution of working
- 690 groups I, II and III to the sixth assessment report of the intergovernmental panel on climate
- change, The Australian National University, 2023.
- 692 Li, C.: The DNDC Model, in: Evaluation of Soil Organic Matter Models, edited by: Powlson, D.
- 693 S., Smith, P., and Smith, J. U., Springer Berlin Heidelberg, Berlin, Heidelberg, 263–267,
- 694 https://doi.org/10.1007/978-3-642-61094-3 20, 1996.
- 695 Lolu, A. J., Ahluwalia, A. S., Sidhu, M. C., Reshi, Z. A., and Mandotra, S. K.: Carbon
- 696 Sequestration and Storage by Wetlands: Implications in the Climate Change Scenario, in:
- Restoration of Wetland Ecosystem: A Trajectory Towards a Sustainable Environment, edited by:
- 698 Upadhyay, A. K., Singh, R., and Singh, D. P., Springer Singapore, Singapore, 45–58,
- 699 https://doi.org/10.1007/978-981-13-7665-8 4, 2020.
- 700 López, D., Sepúlveda, M., and Vidal, G.: Phragmites australis and Schoenoplectus californicus
- in constructed wetlands: Development and nutrient uptake, J. Soil Sci. Plant Nutr., 16, 763–777,
- 702 2016.

- Lund, J., Hanak, E., Fleenor, W., Bennett, W., and Howitt, R.: Comparing futures for the
- 704 Sacramento, San Joaquin delta, Univ of California Press, 2010.
- Mack, S. K., Lane, R. R., Deng, J., Morris, J. T., and Bauer, J. J.: Wetland carbon models:
- Applications for wetland carbon commercialization, Ecol. Model., 476, 110228, 2023.
- Matthes, J. H., Sturtevant, C., Oikawa, P., Chamberlain, S. D., Szutu, D., Arias-Ortiz, A.,
- Verfaillie, J., and Baldocchi, D.: AmeriFlux AmeriFlux US-Myb Mayberry Wetland, Lawrence
- 709 Berkeley National Laboratory (LBNL), Berkeley, CA (United States ..., 2016.
- 710 Meyer, H. and Pebesma, E.: Machine learning-based global maps of ecological variables and
- 711 the challenge of assessing them, Nat. Commun., 13, 2208, 2022.
- 712 Miller, R. L., Fram, M., Fujii, R., and Wheeler, G.: Subsidence reversal in a re-established
- 713 wetland in the Sacramento-San Joaquin Delta, California, USA, San Franc. Estuary Watershed
- 714 Sci., 6, 2008.
- 715 Mitsch, W. J. and Gosselink, J. G.: Wetlands, John wiley & sons, 2015a.
- 716 Mitsch, W. J. and Gosselink, J. G.: Wetlands, John wiley & sons, 2015b.
- 717 Mitsch, W. J., Bernal, B., Nahlik, A. M., Mander, Ü., Zhang, L., Anderson, C. J., Jørgensen, S.
- 718 E., and Brix, H.: Wetlands, carbon, and climate change, Landsc. Ecol., 28, 583–597, 2013.
- 719 Moomaw, W. R., Chmura, G. L., Davies, G. T., Finlayson, C. M., Middleton, B. A., Natali, S. M.,
- 720 Perry, J. E., Roulet, N., and Sutton-Grier, A. E.: Wetlands In a Changing Climate: Science,
- 721 Policy and Management, Wetlands, 38, 183–205, https://doi.org/10.1007/s13157-018-1023-8,
- 722 2018.
- Nahlik, A. M. and Fennessy, M. S.: Carbon storage in US wetlands, Nat. Commun., 7, 1–9,
- 724 2016.
- 725 Nelson, J. A., Walther, S., Gans, F., Kraft, B., Weber, U., Novick, K., Buchmann, N.,
- 726 Migliavacca, M., Wohlfahrt, G., and Šigut, L.: X-BASE: the first terrestrial carbon and water flux
- 727 products from an extended data-driven scaling framework, FLUXCOM-X, Biogeosciences, 21,
- 728 5079–5115, 2024.
- Novick, K. A., Biederman, J. A., Desai, A. R., Litvak, M. E., Moore, D. J., Scott, R. L., and Torn,
- 730 M. S.: The AmeriFlux network: A coalition of the willing, Agric. For. Meteorol., 249, 444–456,
- 731 2018.
- 732 Oh, M., Lee, J., Kim, J., and Kim, H.: Machine learning-based statistical downscaling of wind
- resource maps using multi-resolution topographical data, Wind Energy, 25, 1121–1141,
- 734 https://doi.org/10.1002/we.2718, 2022.
- Ouyang, Z., Jackson, R. B., McNicol, G., Fluet-Chouinard, E., Runkle, B. R., Papale, D., Knox,
- 736 S. H., Cooley, S., Delwiche, K. B., and Feron, S.: Paddy rice methane emissions across
- 737 Monsoon Asia, Remote Sens. Environ., 284, 113335, 2023.
- 738 Parton, W. J., Hartman, M., Ojima, D., and Schimel, D.: DAYCENT and its land surface
- rightarrow submodel: description and testing, Glob. Planet. Change, 19, 35–48, 1998.

- Pastorello, G., Trotta, C., Canfora, E., Chu, H., Christianson, D., Cheah, Y.-W., Poindexter, C.,
- 741 Chen, J., Elbashandy, A., and Humphrey, M.: The FLUXNET2015 dataset and the ONEFlux
- processing pipeline for eddy covariance data, Sci. Data, 7, 225, 2020.
- Peltola, O., Vesala, T., Gao, Y., Räty, O., Alekseychik, P., Aurela, M., Chojnicki, B., Desai, A.
- R., Dolman, A. J., and Euskirchen, E. S.: Monthly gridded data product of northern wetland
- methane emissions based on upscaling eddy covariance observations, Earth Syst. Sci. Data,
- 746 11, 1263–1289, 2019.
- Perry, G. L. W., Seidl, R., Bellvé, A. M., and Rammer, W.: An Outlook for Deep Learning in
- 748 Ecosystem Science, Ecosystems, 25, 1700–1718, https://doi.org/10.1007/s10021-022-00789-y,
- 749 2022.
- Raissi, M., Perdikaris, P., and Karniadakis, G. E.: Physics-informed neural networks: A deep
- 751 learning framework for solving forward and inverse problems involving nonlinear partial
- 752 differential equations, J. Comput. Phys., 378, 686–707, 2019.
- Räsänen, A., Manninen, T., Korkiakoski, M., Lohila, A., and Virtanen, T.: Predicting catchment-
- scale methane fluxes with multi-source remote sensing, Landsc. Ecol., 36, 1177–1195,
- 755 https://doi.org/10.1007/s10980-021-01194-x, 2021.
- Rey-Sanchez, C., Wharton, S., Vilà-Guerau De Arellano, J., Paw U, K. T., Hemes, K. S.,
- Fuentes, J. D., Osuna, J., Szutu, D., Ribeiro, J. V., Verfaillie, J., and Baldocchi, D.: Evaluation of
- 758 Atmospheric Boundary Layer Height From Wind Profiling Radar and Slab Models and Its
- Responses to Seasonality of Land Cover, Subsidence, and Advection, J. Geophys. Res.
- 760 Atmospheres, 126, e2020JD033775, https://doi.org/10.1029/2020JD033775, 2021.
- Saunois, M., Martinez, A., Poulter, B., Zhang, Z., Raymond, P., Regnier, P., Canadell, J. G.,
- Jackson, R. B., Patra, P. K., and Bousquet, P.: Global Methane Budget 2000–2020, Earth Syst.
- 763 Sci. Data Discuss., 2024, 1–147, 2024.
- Sharma, S. and Singh, P.: Wetlands conservation: Current challenges and future strategies,
- 765 John Wiley & Sons, 2021.
- Stewart, G. A., Sharp, S. J., Taylor, A. K., Williams, M. R., and Palmer, M. A.: High spatial
- variability in wetland methane fluxes is tied to vegetation patch types, Biogeochemistry,
- 768 https://doi.org/10.1007/s10533-024-01188-2, 2024.
- 769 Tashman, L. J.: Out-of-sample tests of forecasting accuracy: an analysis and review, Int. J.
- 770 Forecast., 16, 437–450, 2000.
- 771 Tramontana, G., Jung, M., Schwalm, C. R., Ichii, K., Camps-Valls, G., Ráduly, B., Reichstein,
- 772 M., Arain, M. A., Cescatti, A., and Kiely, G.: Predicting carbon dioxide and energy fluxes across
- 773 global FLUXNET sites with regression algorithms, Biogeosciences, 13, 4291–4313, 2016.
- 774 Uhran, B. R., Windham-Myers, L., Bliss, N. B., Nahlik, A., Sundquist, E. T., and Stagg, C. L.:
- 775 Harmonizing wetland soil organic carbon datasets to improve spatial representation of 2011 soil
- carbon stocks in the conterminous United States, https://doi.org/10.5066/P9H1PIX3, 2022.
- 777 Upadhyay, A. K., Singh, R., and Singh, D. P. (Eds.): Restoration of Wetland Ecosystem: A
- 778 Trajectory Towards a Sustainable Environment, Springer Singapore, Singapore,

- 779 https://doi.org/10.1007/978-981-13-7665-8, 2020.
- 780 Valach, A., Shortt, R., Szutu, D., Eichelmann, E., Knox, S., Hemes, K., Verfaillie, J., and
- 781 Baldocchi, D.: AmeriFlux AmeriFlux US-Tw1 Twitchell Wetland West Pond, Lawrence Berkeley
- 782 National Laboratory (LBNL), Berkeley, CA (United States ..., 2016.
- Vaswani, A.: Attention is all you need, Adv. Neural Inf. Process. Syst., 2017.
- 784 Villa, J. A. and Bernal, B.: Carbon sequestration in wetlands, from science to practice: An
- overview of the biogeochemical process, measurement methods, and policy framework, Ecol.
- 786 Eng., 114, 115–128, 2018.
- Weiler, D. A., Tornquist, C. G., Zschornack, T., Ogle, S. M., Carlos, F. S., and Bayer, C.:
- Daycent simulation of methane emissions, grain yield, and soil organic carbon in a subtropical
- 789 paddy rice system, Rev. Bras. Ciênc. Solo, 42, e0170251, 2018.
- 790 Whiting, G. J. and Chanton, J. P.: Primary production control of methane emission from
- 791 wetlands, Nature, 364, 794–795, 1993.
- Windham-Myers, L., Bergamaschi, B., Anderson, F., Knox, S., Miller, R., and Fujii, R.: Potential
- 793 for negative emissions of greenhouse gases (CO2, CH4 and N2O) through coastal peatland re-
- 794 establishment: Novel insights from high frequency flux data at meter and kilometer scales,
- 795 Environ. Res. Lett., 13, 045005, 2018.
- 796 Wood, D. A.: Machine learning and regression analysis reveal different patterns of influence on
- 797 net ecosystem exchange at two conifer woodland sites, Res. Ecol., 4, 24–50, 2022.
- 798 Workgroup, C. W. M.: EcoAtlas, 2019.
- 799 Xu, X. and Trugman, A. T.: Trait-Based Modeling of Terrestrial Ecosystems: Advances and
- 800 Challenges Under Global Change, Curr. Clim. Change Rep., 7, 1–13,
- 801 https://doi.org/10.1007/s40641-020-00168-6, 2021.
- 802 Xu, Y., Liu, X., Cao, X., Huang, C., Liu, E., Qian, S., Liu, X., Wu, Y., Dong, F., and Qiu, C.-W.:
- Artificial intelligence: A powerful paradigm for scientific research, The Innovation, 2, 2021.
- Yao, S., Chen, C., Chen, Q., Zhang, J., and He, M.: Combining process-based model and
- machine learning to predict hydrological regimes in floodplain wetlands under climate change, J.
- 806 Hydrol., 626, 130193, 2023.
- 807 Yin, X., Jiang, C., Xu, S., Yu, X., Yin, X., Wang, J., Maihaiti, M., Wang, C., Zheng, X., and
- 808 Zhuang, X.: Greenhouse gases emissions of constructed wetlands: mechanisms and affecting
- 809 factors, Water, 15, 2871, 2023.
- 810 Yuan, K., Zhu, Q., Li, F., Riley, W. J., Torn, M., Chu, H., McNicol, G., Chen, M., Knox, S., and
- 811 Delwiche, K.: Causality guided machine learning model on wetland CH4 emissions across
- 812 global wetlands, Agric. For. Meteorol., 324, 109115, 2022.
- Yuan, K., Li, F., McNicol, G., Chen, M., Hoyt, A., Knox, S., Riley, W. J., Jackson, R., and Zhu,
- 814 Q.: Boreal–Arctic wetland methane emissions modulated by warming and vegetation activity,
- 815 Nat. Clim. Change, 14, 282–288, 2024.

- Yvon-Durocher, G., Allen, A. P., Bastviken, D., Conrad, R., Gudasz, C., St-Pierre, A., Thanh-
- Duc, N., and Del Giorgio, P. A.: Methane fluxes show consistent temperature dependence
- across microbial to ecosystem scales, Nature, 507, 488–491, 2014.
- 819 Zhang, Y., Li, C., Trettin, C. C., Li, H., and Sun, G.: An integrated model of soil, hydrology, and
- vegetation for carbon dynamics in wetland ecosystems, Glob. Biogeochem. Cycles, 16,
- 821 https://doi.org/10.1029/2001GB001838, 2002.
- 822 Zou, H., Chen, J., Li, X., Abraha, M., Zhao, X., and Tang, J.: Modeling net ecosystem exchange
- of CO2 with gated recurrent unit neural networks, Agric. For. Meteorol., 350, 109985, 2024.

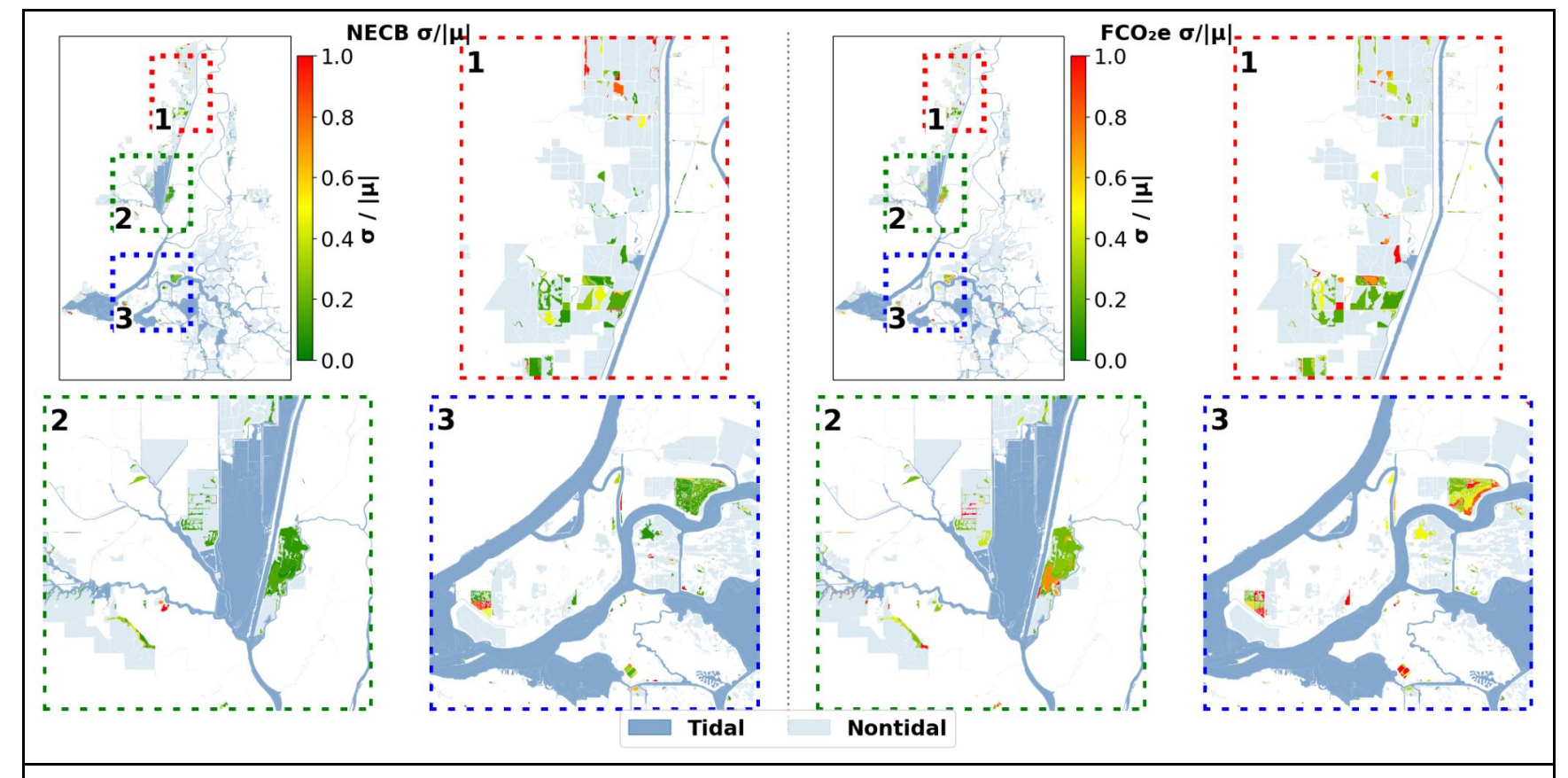


Figure A1: Coefficient of variation $(\sigma/|\mu|)$ of NECB (left) and FCO2e (right) across the 10 runs, showing relative inter-model uncertainty in the predictions. Green areas show high model confidence and red areas shower either lower model confidence (or division by small μ). This can be interpreted as a proxy for the confidence of the spatial upscaling.